A LIGHTWEIGHT MILLET DOWNY MILDEW SPORE DETECTION METHOD BASED ON IMPROVED YOLOv8s
/
基于改进 Yolov8s 的轻量化谷子白发病孢子检测方法

Jianglin YAN[1]; Zhengkun ZHAI[1]; Zhixiang FENG [1]; Lijun CHENG*[1]; Jie YANG*[2 3]
[1] College of Software, Shanxi Agricultural University, Shanxi / China;
[2] College of Health Service and Management, Shanxi University of Traditional Chinese Medicine, Shanxi / China;
[3] National International Joint Research Center for Molecular Chinese Medicine, Shanxi Key Laboratory of Chinese Medicine Encephalopathy, Shanxi University of Chinese Medicine, Shanxi / China;
Correspondent authors: Lijun CHENG: Tel: 13835441585; E-mail: cljzyb@sxau.edu.cn;
Jie YANG: Tel: 13623620021; E-mail: yjsxtcm@sxtcm.edu.cn
DOI: https://doi.org/10.35633/inmateh-75-27

***Keywords:** Deep learning, millet downy mildew, spores, target detection, YOLOv8s*

ABSTRACT

This paper proposes a lightweight spore detection method for millet downy mildew based on an improved YOLOv8s, aiming to enhance the accuracy and efficiency of spore detection. First, the backbone network of the YOLOv8s model was modified by replacing the original backbone with EfficientViT. The substitution of the EfficientViT backbone enables global receptive field and multi-scale learning, which helps to reduce computational costs. While maintaining high performance, this modification significantly improves computational efficiency. Second, a Frequency-Adaptive Dilated Convolution (FADC) module was added to the neck of the model. By adaptively adjusting the receptive field of dilated convolution, the FADC module optimizes the detection of different frequency information. It improves the detection of small objects without adding extra computational burden. Finally, the detection head was optimized to better adapt to the task of detecting millet downy mildew spores, resulting in enhanced detection speed and accuracy. The improved algorithm, named EFP-YOLOv8s, maintains the same mAP50 as the original YOLOv8s model while reducing the number of parameters by 37.8% and computational cost by 58.5%. By balancing high performance with reduced computational resource demands, the model achieves lightweight design, making it more deployable and scalable in practical applications.

摘要

本文提出了一种基于改进 YOLOv8s 的轻量化谷子白发病孢子检测方法，旨在提高孢子检测的准确性和效率。首先，针对 YOLOv8s 模型的主干网络进行了改进，将原有的主干网络替换为 EfficientViT。通过替换主干网络 EfficientViT 实现全局感受野和多尺度学习，有助于降低计算成本。在保持高性能的同时，显著提高了计算效率。其次，在模型的颈部添加了 FADC（Frequency-Adaptive Dilated Convolution）模块，通过自适应地调整膨胀卷积的感受野，针对不同频率的信息进行优化。在不增加额外计算量的同时改善小目标的检测效果。最后，对检测头进行了优化，使其更加适应谷子白发病孢子的检测任务，提高了检测速度和准确性。改进后的算法 EFP-YOLOv8s 相比原 YOLOv8s 模型 mAP50 保持不变，参数量下降 37.8%，计算量下降 58.5%。该模型在保持高性能的同时，也降低了计算资源的需求，实现轻量化，更易于在实际应用中部署和推广。

INTRODUCTION

Millet downy mildew is a soil-borne and seed-borne systemic disease caused by **Sclerospora graminicola (Wang et al., 2024)*. This disease affects the normal growth of cereal leaves and aggravates the tendency of leaf rot. It usually occurs at the 3-leaf stage of seedlings, and at the early stage of the disease, white spots are produced on the adaxial surface of the leaves, accompanied by a moldy layer on the dorsal surface with a grayish-white color, and the diseased grains show a leaflet shape *(Cheng et al., 2020)*. During different growth stages after millet is infected, the disease manifests symptoms such as gray back, white tip, spear-like stalk, white hair, and hedgehog head. The brown powdery substance observed in these symptoms is the oospores of the downy mildew fungus *(Yan et al., 2019)*. These oospores can rapidly multiply and infect plants under suitable conditions, leading to a significant decrease in grain yield and even causing crop failure *(Yue et al., 2021)*. Therefore, timely and accurate detection of cereal white disease spores is of great significance in preventing and controlling the spread of the disease and ensuring the stability and safety of cereal production.

In the early stage, spore detection and counting mainly relied on manual observation and counting, such as hemocyte counting method and plate colony counting method *(Li et al., 2006)*. Although these methods can reflect the number of spores to a certain extent, they are cumbersome, time-consuming and laborious to operate, and the operation error between different personnel is large, which makes it difficult to meet the demand for high-precision and high-volume detection. To overcome these limitations, researchers began to explore more efficient and accurate counting methods. Spore counting methods based on PCR technology are highly accurate, but the operation is complicated, costly and also time-consuming *(Wang et al., 2024)*. In recent years, spore detection and counting methods based on emerging technologies such as fluorescent labeling, flow cytometry, and molecular chemistry have emerged *(Liu et al., 2023; Ren et al., 2022; Aguayo et al., 2018)*. These techniques not only significantly improve the sensitivity and specificity of spore detection, but more importantly, they are able to achieve high-precision quantification of spore counts, providing more reliable data support for scientific research and practical applications.

With the rapid development of computer vision and deep learning technology, image-based target detection methods show great potential in the field of plant disease detection. In 2018, the K-means clustering algorithm was used for image segmentation, image preprocessing, identification of contacted downy spores based on shape factor and area of the spores, and contacted downy spore outline segmentation based on the combination of concavity and contour segmentation. This approach aimed to achieve accurate and automatic detection and counting of spores *(Lei et al., 2018)*. In 2020, an improved U-Net architecture was proposed, reaching a segmentation rate of 91.4%. The new network architecture achieved a higher segmentation rate in the segmentation task of the wheat powdery mildew spore image dataset *(Liang et al., 2020)*. In 2023, a spin-up UNet++ feature extraction network was constructed, with an average recognition accuracy of 99.03%, which improved the segmentation rate by 10.35 percentage points compared to the original CenterNet model *(Zhou J. et al., 2023)*. In 2024, microscopic image processing and machine learning techniques were used to help identify spores of a fungus that can be used to infect pathogens. The method extracted texture, color and shape features of the spores and classified them using Random Forest algorithm with an accuracy of 95.38% *(Nezhad et al., 2024)*.

The YOLO (You Only Look Once) series of algorithms, with its high efficiency and accuracy, has achieved remarkable results in real-time target detection tasks. In 2020, it was proposed for Yolov3 algorithm to join the traditional morphological processing of spore recognition method in microscope images. The accuracy of the spore recognition algorithm increased to more than 94%, and the detection rate was more than 82% *(Li X. et al., 2020)*. In 2023, the number of parameters and computation of the model were reduced by incorporating FasterNet and NAM attention mechanism module into the base model YOLOv5m. It effectively improved the speed and accuracy of spore detection of cucumber downy mildew fungus *(Qiao C. et al., 2023)*. In addition, the Ghost convolution of CBAM attention mechanism was introduced to replace the CSP structure, improving the feature fusion network and utilizing a finer-grained mesh for the detection of dense and sticky small targets. The loss function was enhanced by assigning different weights to various output feature maps, and DIoU_NMS was used instead of NMS *(Li M. et al., 2023)*. In 2024, a small target detection layer was added to the original Yolov8 model, incorporating the focal attention mechanism and WIoU loss function. The average detection accuracy mAP @ 0.5 in the spore data set reached 96.8 % *(Zhang D. et al., 2024)*. Additionally, the backbone network of the original YOLOv8 model was replaced with PP-LCNet, the EMA attention mechanism module was introduced in the neck network, and the bounding box loss function was replaced with WIOU. These modifications reduced the number of floating-point operations per second while maintaining higher detection accuracy *(Luo B. et al, 2024)*.

Traditional deep learning models often suffer from high computational complexity, large number of parameters, and slow inference speed, making it difficult to meet the demand for real-time detection and mobile deployment in agricultural scenarios. Therefore, it is of great practical significance to improve the YOLO series of algorithms in a lightweight way. In 2024, the CG module was added to the original backbone of YOLOv5s along with the HS-FPN module, resulting in a significant reduction in the number of model parameters and accurate detection of various types of pathogen spores. YOLOv8s optimized feature extraction capability compared to YOLOv5, improving detection accuracy while maintaining a relatively lightweight structure (*Cheng et al., 2024*). Additionally, by introducing GhostConv to replace standard convolution, constructing the LightC3 module, adopting BiFPN instead of the Concat operator, and integrating the SE attention mechanism, the computational burden and the number of model parameters were significantly reduced while maintaining high detection accuracy (*Meng F. et al., 2024*).

A study for wheat grain counting achieved efficient detection and counting in complex scenarios by improving the YOLOv8's neck network into a BiFPN structure, further validating the effectiveness of the lightweight design (*Ma N. et al., 2024*).

Given the characteristics of small, dense, and clustered targets in millet downy mildew spore images, as well as the relatively high computational costs and parameter counts of the aforementioned improved networks that hinder deployment, this study develops a lightweight detection model for millet downy mildew spores by integrating an EfficientNet-ViT backbone, a C2f_FADC neck module, and an optimized detection head. This model not only achieves excellent detection performance but also enables accurate identification of pathogen spores while maintaining high efficiency. It is anticipated that the findings of this study will provide robust support for the prevention and control of millet downy mildew and contribute to the advancement of intelligent and precise agriculture.

MATERIALS AND METHODS

Image Data Acquisition

First, millet plants with typical symptoms of downy mildew were selected from the field. The mature diseased panicles were excised using sterile scissors as samples. These samples were then filtered through a 0.04 mm mesh sieve to remove large particulate impurities from the suspension. Next, the collected diseased tissue sample was placed into a centrifuge tube containing an appropriate amount of sterile water, and the spores were fully shaken using a vortex shaker to disperse the spores in suspension as evenly as possible. Finally, an appropriate amount of spore suspension droplets was added to the microscope slide, and the coverslip was placed under the microscope, and the number of oospores in the field of view was observed under the microscope at 10×10 times the microscope. A total of 2042 images were obtained, with a resolution of 1800 pixels × 1350 pixels, in jpg format.

Image Preprocessing

The acquired spore images showed significant dense distribution and adhesion characteristics, which posed a challenge to the subsequent spore identification and counting work. In this paper, the methods of randomly adjusting saturation, adding Gaussian noise and changing brightness are used to simulate the complex and changeable environmental conditions in the field and various lighting conditions, shooting angles and noise interference factors that may be encountered in the actual detection scene, aiming to expand the data set from multiple dimensions. A total of 6126 images were obtained after expansion. The dataset was divided into a training set of 4926 sheets and a validation set of 1200 sheets according to the ratio of 8:2.

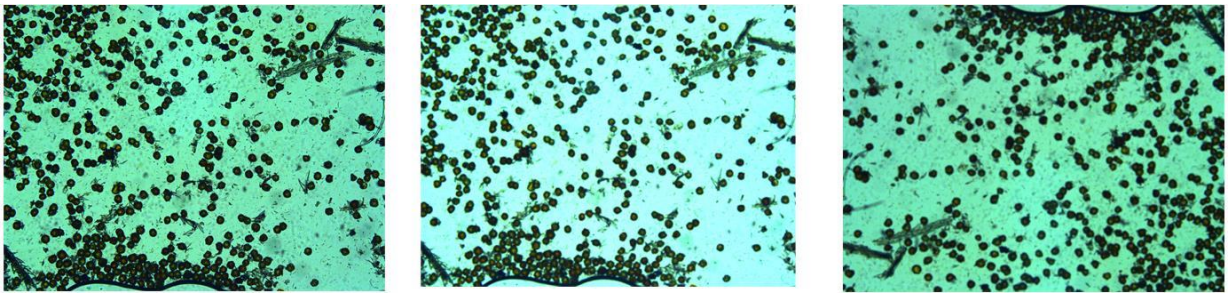

a) **b)** **c)**

Fig. 1 - Microscopic images of millet downy mildew spores

a) Original image; b) Adjusted saturation and brightness; c) Adding Gaussian noise and flipping

YOLOv8s model structure

YOLOv8 is a YOLO target detection and image segmentation model developed by Ultralytics *(Redmon J. et al., 2016)*. YOLOv8 introduces an Anchor-Free detection head, a new loss function, and a Task-AlignedAssigner positive and negative sample allocation strategy to improve the detection accuracy and speed of the model. In addition, YOLOv8 provides models with different scales, such as Nano, Small, Medium, Large and ExtraLarge, where YOLOv8x is the most accurate but runs the slowest with the largest model size, and YOLOv8n is the fastest with the smallest model size. Considering the accuracy and speed requirements of spore detection in real scenarios, YOLOv8s in YOLOv8 is chosen as the benchmark model for improvement.

Improvement of YOLOv8s model

First, the backbone network of the YOLOv8s model was improved by replacing the original backbone network with EfficientViT. EfficientViT combines the advantages of convolutional neural network (CNN) and Transformer, which has stronger feature extraction capability and higher computational efficiency, thus enhancing the accuracy of spore detection. Secondly, the FADC module is added to the neck of the model, which enhances the model's ability to learn spore features by introducing the attention mechanism, further improving the accuracy of detection.Finally, the detection head was optimized to better adapt to the task of detecting millet downy mildew spores, resulting in improved detection speed and accuracy.

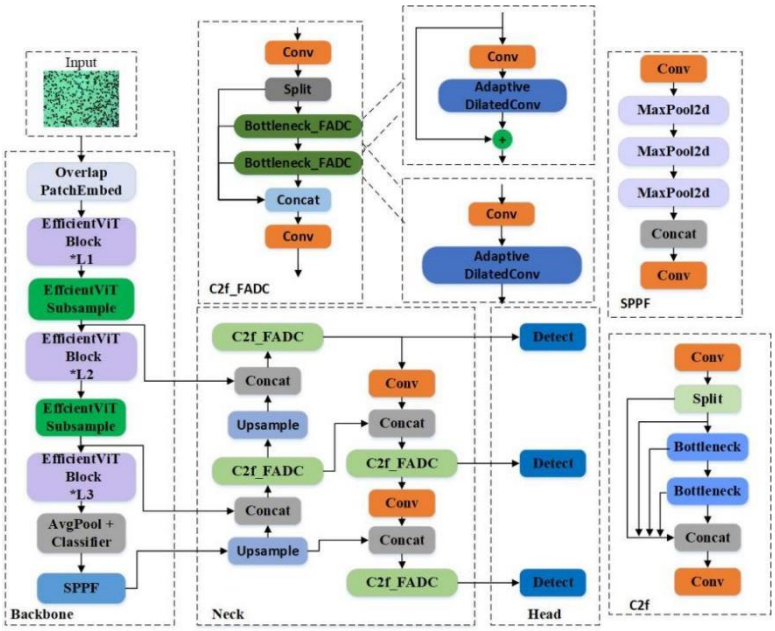

Fig. 2 - EFP-YOLOv8 model

EfficientVit

EfficientVit consists of three phases, each containing a number of sandwich structures, which are composed of 2N DWConv (spatially localized communication) and FFN (channel communication) as well as cascaded packet attention *(Liu et al., 2023)*. Compared with the traditional Multi-Headed Self-Attention (MHSA), CGA performs head segmentation of the features before generating the query (Q), key (K) and value (V). This change not only improves the efficiency of computation, but also allows each head to focus on a different subset of features, thus enhancing the diversity and expressiveness of the model. To further enhance the model capacity, EfficientViT sums the output of each head with the input of the next head, realizing the effective transfer and fusion of feature information. Eventually, the outputs of multiple heads are stitched together and mapped through a linear layer to obtain the final output features.

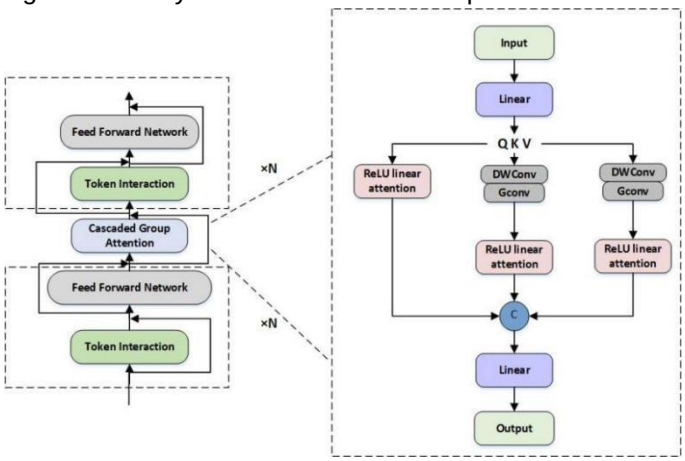

Fig. 3 - EfficientViT network structure diagram

In the Cascaded Grouped Attention (CGA) approach, the model splits the complete feature into multiple parts and provides these parts to each head separately for processing. This way of partitioning features not only saves computation, but also makes the attention computation more efficient.

Each head focuses on processing a different subset of features, which improves the diversity and robustness of the model. The computational formulas are shown in Eq. (1) to Eq. (3).

$$\widetilde{X}_{mn}=Attn(X_{mn}Y^{Q}_{mn,}\ X_{mn}Y^{K}_{mn,}\ X_{mn}Y^{V}_{mn} \quad (1)$$

$$\widetilde{X_{m+1}} = Con[\widetilde{X_{mn}}]_{n=1:h}Y^{P}_{m} \quad (2)$$

$$X'_{mn} = X_{mn} + \tilde{X}_{m(n-1)}, 1 < n \leq h \quad (3)$$

X_{mn} is the *n*-th partition of the input feature X_m, X_m =[$X_{m1,}$ $X_{m2,...,}X_{mh}$], $1<n\leq h$, is the total number of heads, Y^{Q}_{mn}, Y^{K}_{mn}, and Y^{V}_{mn} are projection layers that partition the input features into different subspaces and Y^{P}_{m} is a linear layer that projects the connected output features with the same dimension as the input. X'_{mn} is the residual connection of the *m*-th head output and input.

C2F_FADC

The C2f module in YOLOv8 realizes the fusion of feature maps at different scales and improves the target detection performance by introducing the ELAN attention mechanism and Bottleneck design. The C2f_FADC module further introduces the attention mechanism and the deep convolution based on this foundation, which optimizes the computational efficiency of the model and enhances the focus on the key regions, improving the accuracy and robustness of the model in the complex scenario of the detection performance in complex scenes.

Frequency Adaptive Dilation Convolution (FADC) consists of three strategies: adaptive dilation rate (AdaDR), adaptive kernel (AdaKern), and frequency selection (FreqSelect) (*Chen L. et al., 2024*). AdaDR adjusts the dilation rate spatially, AdaKern operates on the convolution kernel weights, and FreqSelect directly balances the frequency power of the input features in order to encourage the acceptance of domain expansion.

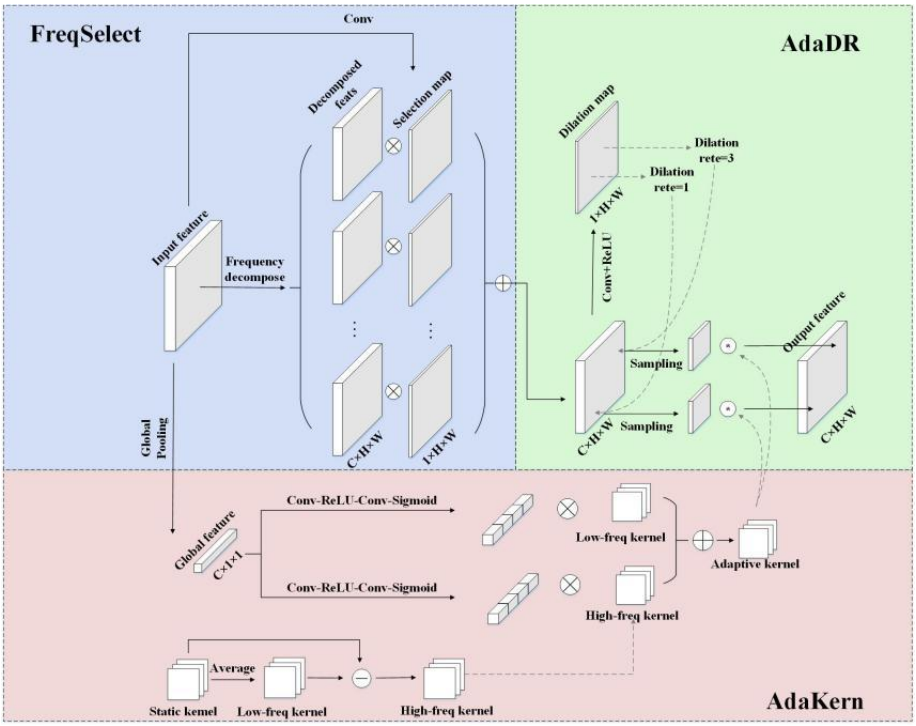

Fig. 4 - FADC network structure diagram

Adaptive Dilation Rate (AdaDR): Unlike the traditional fixed dilation rate, FADC can dynamically adjust the dilation rate according to the frequency characteristics of different image regions. In high-frequency regions, the FADC selects a smaller expansion rate to capture more detailed edge information, while in low-frequency regions, a larger expansion rate can be selected to expand the sensory field.

Adaptive Kernel (AdaKern): This module decomposes the convolutional weights into low-frequency and high-frequency components and dynamically adjusts the ratio between these components on a per-channel basis. By increasing the high-frequency portion of the convolutional weights, AdaKern is able to capture more high-frequency components, thereby increasing the effective bandwidth.

FreqSelect: The FreqSelect module optimally balances high-frequency and low-frequency components in the feature representation by re-weighting the spatial variance. It suppresses high-frequency components in the background to encourage the FADC to learn larger expansions, thereby expanding the range of the receptive field.

Detection head improvements

The main function of the detection head is to process the input feature map to detect targets in the image. It integrates and analyzes features of different levels and scales through techniques such as multi-scale feature fusion, thus adapting to the detection of targets of different sizes. In order to further reduce the number of model parameters without decreasing the detection accuracy, this paper introduces a local convolutional neural network PConv, so that the two convolutional branch inputs of the detection head share the same PConv and the output feature maps of the 1×1 Conv, which achieves the reduction of computational redundancy, and at the same time facilitates the effective sharing and utilization of features among different branches to optimize the performance and efficiency of the detection head.

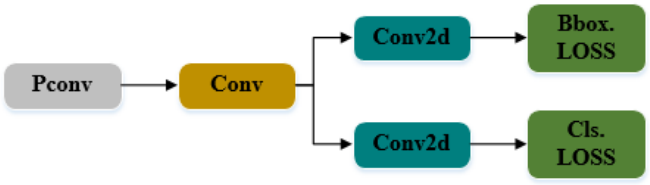

Fig. 5 -Detect structure diagram

PConv optimizes performance by reducing redundant memory accesses. When dealing with continuous or regular memory accesses, PConv can selectively apply a convolutional kernel that performs spatial feature extraction for only a portion of the input channel and leaves the remaining channels unchanged. This strategy significantly reduces memory accesses.

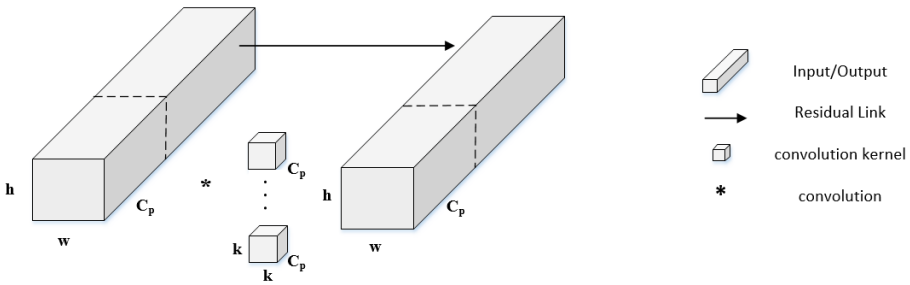

$$FLOPS = h \times w \times k_2 \times C_p^2$$

Fig. 6 - PConv structure diagram

The number of floating point operations FLOPs for PConv convolution is:

(6)

where h represents the height of the feature map; w represents the width; k represents the size of the convolution kernel; and represents the number of channels. the number of floating-point operations for PConv convolution is only 1/16 of that for regular Conv convolution.

RESULTS

Parameter Configuration and Evaluation Indicators

For the hardware environment configuration, the CPU is Intel(R)Core(TM)i9-9900KFCPU@3.60GHz, the GPU model is Quadro P5000, the host memory is 125GB, and the video memory is 16GB. For the software environment setup, the 64-bit Linux operating system is used, and the programming language used is Python3.8. CUDA11.0 was used to complete the computational acceleration, and the deep learning framework Pytorch1.8.1 was used for training. The specific training parameters in the experiment are set as follows, the

resolution of the input image (image_size) is 640×640 pixels, the initial learning rate (learning_rate) is set at 0.01, the batch size (batch_size) is set at 16, and the number of iterations (epochs) is 100.

In this paper, the accuracy rate (Precision, P), meanAveragePrecision (mAP), the size of model parameters (Parameters), and the amount of model computation (GFLOPS) are used to evaluate the performance of the model.

The formula for each metric is as follows:

$$P = \frac{TP}{TP+FP} \tag{7}$$

$$R = \frac{TP}{TP+FN} \tag{8}$$

$$AP = \int_0^1 P(R)dr \tag{9}$$

$$mAP = \frac{1}{n}\sum_{i=1}^{n} AP_i mAP = \frac{1}{n}\sum_{i=1}^{n} AP_i \tag{10}$$

In the formula TP is the number of spores correctly detected; FP is the number of background impurities mistakenly detected as spores; FN is the number of spores identified as impurities; R is the value of the recall rate under the current accuracy rate, which refers to the proportion of spores detected by the model to all actual spores; the area under the P-R curve plotted using the precision rate P and the recall rate R represents the average precision AP value of the category. The higher the AP value, the better the detection performance of the algorithm is considered to be.

Backbone network comparison test

In order to evaluate the advantages of replacing the backbone network with EfficientViT, three lightweight models, namely, Efficientnet, GhostNet, and MobileNetV3, are selected as the backbone network of the original model of YOLOv8s for the comparison experiments. The specific experimental results are shown in Table 1.

Table 1

Comparative experiments of different backbone networks

Model	Parameters /MB	GFLOPS	P/%	mAP50/%
YOLOv8s	11.1	28.4	97.1	97.6
YOLOv8s+Efficientnet	10	22.0	97.4	97.1
YOLOv8s+GhostNet	6.3	16.3	95.3	96
YOLOv8s+MobileNetV3	6.6	16.3	96	96.9
YOLOv8s+EfficientViT	8.4	20.4	96.9	97.1

From the analysis in Table 1, replacing the backbone network with GhostNet based on the YOLOv8s model reduces the computation and number of parameters by 4.8 and 12.1, respectively, but the $mAP50$ decreases by 1.8 percentage points. mobileNetV3 decreases in the number of parameters and computation, but decreases in P, $mAP50$, and R. EfficientNet network model has a 9.9% decrease in the number of parameters, a 22.5% decrease in computation, a 0.3 percentage point increase in precision, and decreases in both $mAP50$ and R. EfficientViT has faster detection with a very small decrease in precision, where the number of parameters decreases by about 24.3%, the computation decreases by about 28.2%.

Comparative experiments with different convolutions of the neck

From the analysis in Table 1, the experimental results show that C2f_FADC proposed in this paper performs better in terms of accuracy improvement. The number of C2f_Star_CAA parameters and the computation amount are increased compared to the base model. The introduction of C2f_RFAConv detection accuracy decreases and the computational amount rises, which is not in line with the experimental purpose of

this paper. In summary, the introduction of C2f_FADC not only realizes the lightweighting of the network, but also improves the detection accuracy of the model on the image target to achieve the purpose of the model optimization, which proves the validity of the improved method in this paper.

Table 2

Comparison experiment on different convolutions in neck

Model	Parameters / MB	GFLOPS	P / %	mAP50/%
YOLOv8s+EfficientViT	8.4	20.4	96.9	97.1
YOLOv8s+EfficientViT+C2f_Star_CAA	9.4	22.6	96.6	97.2
YOLOv8s+EfficientViT+C2f_Faster_EMA	7	17.8	96.6	97.4
YOLOv8s+EfficientViT+C2f_RFAConv	8.4	20.6	96.2	96.9
YOLOv8s+EfficientViT+C2f_FADC	8.4	18.7	96.9	97.5

Optimized Detection Head Comparison Experiment

To further achieve lightweighting, PConv, RepConv, EMSConvP, and RepConv are used to improve the detection head, respectively. As can be seen from Table 3, the number of EMSConvP parameters decreases by 19.8%, and the computational volume decreases by 46.1%. the number of RepConv parameters rises, and the computational volume decreases by a small amount. The method using PConv to optimize the detection head compares the base model accuracy and mAP changes are not obvious, but the number of parameters decreases by 37.8% and the computation amount decreases by 58.5%, which is the best lightweight effect in the comparison experiments. The lightweight detection head in this paper has great advantages in model deployment ability and small target detection ability, and has high accuracy and fast calculation speed in grain powdery mildew spore detection.

Table 3

Improved detection head comparison experiment

Model	Parameters / MB	GFLOPS	P / %	mAP50 /%
YOLOv8s	11.1	28.4	97.1	97.6
YOLOv8s+EfficientViT+C2f_FADC	8.4	18.7	96.9	97.5
YOLOv8s+EfficientViT+C2f_FADC+PConv	6.9	11.8	96.8	97.6
YOLOv8s+EfficientViT+C2f_FADC+EMSConvP	8.9	15.3	96.8	97.4
YOLOv8s+EfficientViT+C2f_FADC+RepConv	12.6	22.1	96.8	97.5

Comparison of different models

To further validate the advantages of the EFP-YOLOv8s model proposed in this paper for the detection of millet downy mildew spores, the improved model was compared with YOLO v5s, YOLO v6s, YOLO v8s, YOLOv9s, YOLOv10s, and the final results of the comparison are shown in Table 4. According to the experimental results, it can be seen that the accuracy rate and mAP50 value of each model are relatively close to each other, among which the base model YOLOv8s has the highest accuracy rate of 97.1%, but the number of parameters and the amount of calculation are too large. The improved model EFP-YOLOv8s decreased the accuracy rate by 0.3 percentage points compared with the original model, and the mAP remained unchanged, but the number of parameters decreased by 37.8% and the computational volume decreased by 58.5%. Compared with YOLOv5s, YOLOv6s, YOLOv9s, and YOLOv10s, EFP-YOLOv8s has the best combined accuracy and mAP, and the computational and parametric quantities are lower than the other models.

Table 4

Comparative experiments with different models

Model	Parameters /MB	GFLOPS	P/%	mAP50/%
YOLOv5s	9.1	23.8	96.8	97.5
YOLOv6s	16.3	44	96.9	97.7
YOLOv8s	11.1	28.4	97.1	97.6

YOLOv9s	7.1	26.7	96.7	97.5
YOLOv10s	7.2	21.4	96.7	96.5
EFP-YOLOv8s	6.9	11.8	96.8	97.6

SPORE DETECTION AND TRAINING SYSTEM FOR FOXTAIL MILLET DOWNY MILDEW

In this study, a Sporisorium scitamineum spore detection system based on PyQt5 was developed, which comprises two main functional interfaces: the spore detection and counting interface, and the model training interface.

Spore detection and counting interface

This interface is designed to provide a convenient tool for efficient detection and precise counting of Sporisorium scitamineum spores. Users can select and upload spore image files stored locally through the interface to the system. The system utilizes deep learning algorithms to automatically recognize and label the spores in the images, displaying the labeled images in real-time on the interface. Upon completion of the detection, the interface automatically tallies the number of spores and presents the results clearly in the result display area. Additionally, users have the option to save the labeled images locally.

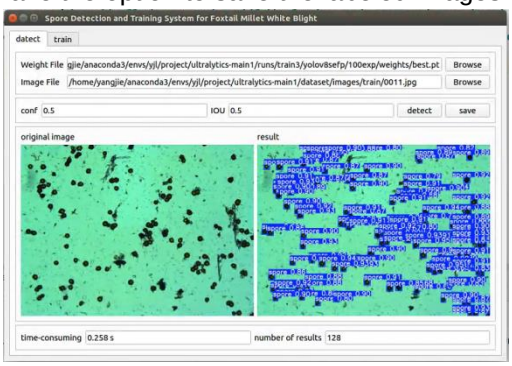

Fig. 7 - Spore detection and counting interface

Model training interface

This interface allows users to import customized spore image datasets for training or optimizing deep learning models. Users can flexibly set training parameters through this interface, such as learning rate, batch size, and number of training epochs, to enhance model performance. During the training process, the interface displays real-time training logs, aiding users in intuitively monitoring the model's training status. Additionally, the interface supports model saving and loading functionalities, enabling users to save trained models locally for direct use in subsequent detection tasks.

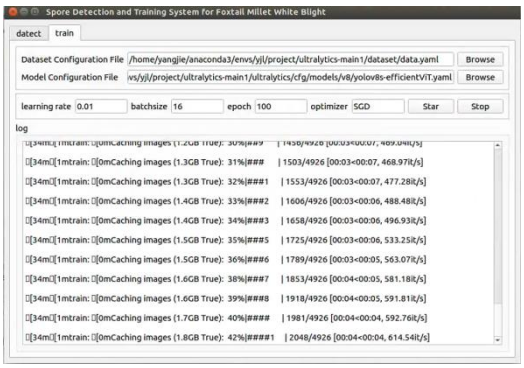

Fig. 8 - Model training interface

CONCLUSIONS

In this paper, a lightweight YOLOv8s model is proposed to replace the backbone network, introduce C2f_FADC and improve the detection head. Through comparative experiments, it is verified that the improved model maintains high precision detection accuracy compared to YOLOv8s while the number of parameters decreases by 37.8% and the computational amount decreases by 58.5%. The improved mAP50 is 97.6% and P reaches 96.8%, which gives certain advantages to the EFP-YOLOv8s model proposed in this paper compared with mainstream target detection networks.

This research result not only provides a new technical means for the prevention and control of cereal leucosis, but also provides ideas and methods that can be used for the detection of disease spores in other crops.

In the future, more advanced lightweight technology and optimization strategies will continue to be explored to further improve the detection performance and practicality of the model, and to promote the continuous development and application of intelligent technology in agriculture.

ACKNOWLEDGEMENT

This research was supported by the Teaching Reform Innovation Project of Higher Education Institutions in Shanxi Province (J20220247) and the Youth Scientific Research Project of the Basic Research Program of Shanxi Province (NO.202303021222039).

REFERENCES

[1] Aguayo, J., Fourrier-Jeandel, C., Husson, C., Ioos, R., (2018). Assessment of Passive Traps Combined with High-Throughput Sequencing to Study Airborne Fungal Communities. *Applied and environmental microbiology*, Vol. 84, United States.

[2] Chen, L., Gu, L., Zheng, D., & Fu, Y., (2024). Frequency-Adaptive Dilated Convolution for Semantic Segmentation. *Proceedings of the IEEE/CVF Conference on Computer Vision and Pattern Recognition*, pp. 3414-3425, United States.

[3] Cheng, F., Wang, H., Han, Y., Han, Y., (2020). Research Advances on Downy Mildew of Foxtail Millet in China (我国谷子白发病研究进展). *Journal of Shanxi Agricultural Sciences*, Vol. 48, pp. 263-267, Shanxi / China.

[4] Cheng, T., Zhang, D., Gu, C., Zhou, X., Qiao, H., Guo, W., & Yang, X., (2024). YOLO-CG-HS: A lightweight spore detection method for wheat airborne fungal pathogens. *Computers and Electronics in Agriculture,* Vol. 227, Netherlands.

[5] Nezhad, S. F., Rahnama, K., Javidan, M. S., & Vakilian, A. K., (2024). Application of microscopic image processing and artificial intelligence detecting and classifying the spores of three novel species of Trichoderma. *Discover Applied Sciences*, Vol. 6, Switzerland.

[6] Redmon, J., Divvala, K. S., Girshick, B. R., & Farhadi, A., (2015). You Only Look Once: Unified, Real-Time Object Detection. *CoRR*, United States.

[7] Lei, Y., Yao, Z., He, D., (2018). Automatic detection and counting of urediniospores of Puccinia striiformis f sp tritici using spore traps and image processing. *Scientific Reports*, Vol. 8, pp. 1-11, England.

[8] Li, A., Yue, S., Ma, H., (2006). Correlativity of three counting methods of fungal spore (真菌孢子三种计数方法相关性的探讨). *Journal of Microbiology*, pp. 107-110, Liaoning/China.

[9] Li, M., Ding, Z., Zhao, J., Chen, S., Li, W., Yang, X., (2023). Detection method for cucumber downy mildew sporangia in a solar greenhouse based on improved YOLOv5s (基于改进 YOLOv5s 的日光温室黄瓜霜霉病孢子囊检测计数方法). *Journal of Chinese Agricultural Mechanization*, Vol. 44, pp. 63-70, Jiangsu/China.

[10] Li, X., Zhao, L., Shao, B., Wang, D., (2020). A new method for spore identification in microscope images based on morphology and Yolov3 algorithm (一种新的基于形态学与 Yolov3 算法的显微镜图像中孢子识别方法). *Intelligent Computer and Applications*, Vol. 10, pp. 30-34+38, Heilongjiang/China.

[11] Liang, X., Wang, B., (2023) Wheat Powdery Mildew Spore Images Segmentation Based on U-Net. *Proceedings of the 2nd International Conference on Artificial Intelligence and Computer Science (AICS 2020*), pp.529-534, Faculty of Information Technology, Beijing University of Technology.

[12] Liu, J., Zhang, M., Ren, S., Wang, Y., Ma, J., Quan, J... & Li, Z., (2023). Genetic Diversity of Pyricularia oryzae Based on SRAP Molecular Markers（利用 SRAP 分子标记分析谷瘟病菌遗传多样性). Ac*ta Agriculturae Boreali-Sinica*, Vol. 38, pp. 179-187, Hebei/China.

[13] Liu, X., Peng, H., Zheng, N., Yang, Y., Hu, H., Yuan, Y., (2023). EfficientVit: Memory efficient vision transformer with cascaded group attention. *Proceedings of the IEEE/CVF Conference on Computer Vision and Pattern Recognition*, pp. 14420-14430, United States.

[14] Luo, B., Li, J., Zhou, Y., Pan, D., Huang, S., (2024). Lightweight Rice Blast Spores Detection Method Based on Improved YOLOv8 (基于改进 YOLOv8 的轻量化稻瘟病孢子检测方法). *Transactions of the Chinese Society for Agricultural Machinery,* Vol. 55, pp. 32-38, Beijing/China.

[15] Ma, N., Li, Z., Kong, Q., (2024). Wheat grains automatic counting based on lightweight YOLOv8. *INMATEH - Agricultural Engineering*, Vol. 73, pp. 592-602, Romania.

[16] Meng, F., Yan, C., Yang, Y., Xing, R., Zhu, D., Zhang, A., & Liao, J., (2024). A lightweight improved YOLOv5s model-based rice blast detection method and mobile deployment. *INMATEH - Agricultural Engineering*, Vol. 74, pp. 771-786, Romania.

[17] Qiao, C., Han, M., Gao, W., Li, K., Zhu, X., Zhang, L., (2023). Quantitative Detection of Cucumber Downy Mildew Spores at Multi-scale Based on Faster-NAM-YOLO (基于 Faster-NAM-YOLO 的黄瓜霜霉病菌孢子检测). *Transactions of the Chinese Society for Agricultural Machinery*, Vol. 54, pp. 288-299, Beijing/China.

[18] Ren, A., Chen, S., Liu, K., Zhao, J., Yang, X., Li, M., (2022). Counting of cucumber downy mildew sporangia based on flow cytometry (基于流式细胞术的黄瓜霜霉病菌孢子囊计数研究). *Acta Phytopathologica Sinica*, Vol. 52, pp. 841-848, Beijing/China.

[19] Wang, A., Shang, Z., Zhang, M., Wang, G., Hu, X., Xu, F... & Zhou, Y., (2024). Dynamic monitoring of aerial conidia and disease estimation models for wheat powdery mildew in fields using pathogen spore traps coupled with real-time PCR technique (基于病菌孢子捕捉和 real-time PCR 技术的田间空气中小麦白粉病菌孢子动态监测及病情估计模型研究). *Plant Protection*, Vol. 50, pp. 49-56+72, Beijing/China.

[20] Wang, Y., Li, H., Tian, G., Liu, X., Liu, H., & Wang, Z., (2024). Problems and Improvement Measures of Foxtail Millet Production in Shanxi Province (山西谷子生产问题及改进措施). *China Seed Industry*, pp. 46-48+55, Beijing/China.

[21] Yan, Y., Xu, Y., He, Z., Gao, J., (2019). Isolation and Identification of the Mycoparasite on Oospores from Scolerospora graminicola (谷子白发病菌卵孢子重寄生真菌的分离与鉴定) . *Journal of Shanxi Agricultural Sciences*, Vol. 47, pp. 891-894+907, Shanxi/China.

[22] Yue, J., Wang, P., Han, Y., Gao, J., (2021). Isolation and Identification of Heavy Parasitic Fungi from the Oospores of Sclerospora graminicola (Sacc.) Schroet (谷子白发病卵孢子重寄生真菌的分离鉴定). *Journal of Shanxi Agricultural Sciences*, Vol. 49, pp. 82-86+104, Shanxi/China.

[23] Zhang, D., Gao, Y., Cheng, T., Hu, G., Yang, X., Qiao, H... & Gu, C., (2024). Detection of wheat scab spores in dense scene based on YOLOv8-FECA (基于 YOLOv8-FECA 的密集场景下小麦赤霉病孢子目标检测). *Transactions of the Chinese Society of Agricultural Engineering*, Vol. 40, pp. 127-136, Beijing/China.

[24] Zhou, J., Chen, P., Lei, Y., Huang, L., Zhao, J., & Liang, D., (2023). Automatic detection of urediniospores method for wheat stripe rust pathogen based on spin UNet++ network (基于自旋式UNet++网络的小麦条锈病菌夏孢子自动检测方法). *Journal of Nanjing Agricultural University*, Vol. 46, pp. 1004-1010, Jiangsu/China.